

# Explaining the possible 95 GeV excesses in the B-L symmetric SSM

Jin-Lei Yang<sup>1,2,3\*</sup>, Ming-Hui Guo<sup>1,2</sup>, Wen-Hui Zhang<sup>1,2</sup>, Hai-Bin Zhang<sup>1,2,3†</sup>, Tai-Fu Feng<sup>1,2,3‡</sup>

*Department of Physics, Hebei University, Baoding, 071002, China<sup>1</sup>*

*Key Laboratory of High-precision Computation and Application of Quantum Field Theory of Hebei Province, Baoding, 071002, China<sup>2</sup>*

*Research Center for Computational Physics of Hebei Province, Baoding, 071002, China<sup>3</sup>*

## Abstract

This study investigates the excesses observed in the diphoton and  $b\bar{b}$  data around 95 GeV within the framework of the  $B - L$  supersymmetric model (B-LSSM). Comparing with the minimal supersymmetric standard model, the B-LSSM incorporates two singlet chiral Higgs bosons which mix with the SM-like Higgs boson due to the gauge kinetic mixing effect. The richer Higgs sector indicates that designating the B-LSSM specific CP-even Higgs state as the lightest Higgs boson has great potential to explain the excesses at around 95 GeV. Considering the two-loop effective potential corrections to the squared Higgs mass matrix, it is found that the signal strengths  $\mu(h_{95})_{\gamma\gamma}$ ,  $\mu(h_{95})_{bb}$  can be described simultaneously in the experimental  $1\sigma$  interval. And the B-LSSM specific parameters  $\tan\beta'$ ,  $B_\eta$ ,  $g_{YB}$ ,  $M_{Z'}$  affect the theoretical predictions on the light Higgs boson masses and signal strengths  $\mu(h_{95})_{\gamma\gamma}$ ,  $\mu(h_{95})_{bb}$  significantly.

Keywords: 95 GeV excesses, B-LSSM, new Higgs states

---

\* jlyang@hbu.edu.cn

† hbzhang@hbu.edu.cn

‡ fengtf@hbu.edu.cn

## I. INTRODUCTION

The discovery of a 125 GeV Higgs boson at the Large Hadron Collider (LHC) in 2012 [1, 2] is one of the most remarkable achievements in theoretical physics, and its properties are consistent well with the standard model (SM) predictions [3, 4] which indicates all of the fundamental particles predicted by the SM are observed. Then identifying whether the detected Higgs boson is the only fundamental scalar particle or part of a new physics (NP) theory with extended Higgs sectors becomes the prime goal of the current LHC programme. Although there is no new scalar was found at the LHC so far, several intriguing excesses in the searches for light Higgs bosons below 125 GeV have been observed with increasing precision in the measurements of Higgs couplings to fermions and gauge bosons.

The results based on both the CMS Run 1 and the first year of CMS Run 2 data for Higgs boson searches in the diphoton final state show a  $2.8\sigma$  local excess at the mass about 95 GeV [5, 6], which is compatible with the latest ATLAS result [7] based on the previously reported result utilizing  $80 \text{ fb}^{-1}$  [8] in the diphoton searches

$$\mu(\Phi_{95})_{\gamma\gamma} = \frac{\sigma(gg \rightarrow \Phi_{95}^{\text{NP}})\text{BR}(\Phi_{95}^{\text{NP}} \rightarrow \gamma\gamma)}{\sigma(gg \rightarrow h_{95}^{\text{SM}})\text{BR}(h_{95}^{\text{SM}} \rightarrow \gamma\gamma)} = 0.18 \pm 0.10. \quad (1)$$

Utilizing the full Run 2 data set, CMS published the results for the Higgs boson searches in the  $\tau^+\tau^-$  channel which show a local significance of  $3.1\sigma$  at a mass value about 95 GeV [9]

$$\mu(\Phi_{95})_{\tau\tau} = \frac{\sigma(gg \rightarrow \Phi_{95}^{\text{NP}})\text{BR}(\Phi_{95}^{\text{NP}} \rightarrow \tau\tau)}{\sigma(gg \rightarrow h_{95}^{\text{SM}})\text{BR}(h_{95}^{\text{SM}} \rightarrow \tau\tau)} = 1.2 \pm 0.5. \quad (2)$$

The analysis on the Higgs boson searches in the diphoton final state by CMS further confirmed the excess at about 95 GeV, and the result reads [10]

$$\mu(\Phi_{95})_{\gamma\gamma} = 0.33_{-0.12}^{+0.19}. \quad (3)$$

In addition, the results measured at the Large Electron Positron (LEP) show a local excess of  $2.3\sigma$  at the invariant mass of  $b\bar{b}$  around 98 GeV<sup>1</sup> [11], which can be expressed in terms of

---

<sup>1</sup> The excess at LEP is broad due to the hadronic  $b\bar{b}$  final state, so this result is also compatible with a scalar resonance at 95 GeV, consistent with the diphoton and ditau excesses. We also take the excess for  $b\bar{b}$  final state at about 95 GeV in the following analysis.

a signal strength as

$$\mu(\Phi_{95})_{b\bar{b}} = 0.117 \pm 0.057. \quad (4)$$

Theoretically, there are numerous discussions on the excesses in NP models. The analysis carried out in Refs. [12–28] indicates that the diphoton rate may be several times larger than its SM prediction for the same scalar mass in the next-to-minimal supersymmetric standard model (NMSSM). In the Two-Higgs doublet model (2HDM) with an additional real singlet (N2HDM), the possibilities of explaining the observed excesses were studied in Refs. [29–37]. The authors of Ref. [38] explored the viability of the radion mixed Higgs to be 125 GeV along with the presence of a light radion which can account for the CMS diphoton excess well in the Higgs radion mixing model. Considering the one-loop corrections to the neutral scalar masses of the  $\mu\nu$ SSM, the authors of Refs. [39, 40] demonstrated how the  $\mu\nu$ SSM can simultaneously accommodate two excesses measured at the LEP and LHC at the  $1\sigma$  level. Based on the analysis in Ref. [41], extending the scalar sector with a  $SU(2)_L$  triplet (the hypercharge  $Y = 0$ ) can well provide the origin of the 95 GeV excesses. Whether certain model realizations could simultaneously explain the two excesses while being in agreement with all other Higgs boson related limits and measurements was reviewed in Refs. [42, 43].

In this work, we investigate the diphoton and  $b\bar{b}$  excesses in the  $B - L$  supersymmetric model (B-LSSM) [44–52]<sup>2</sup>. Compared with the minimal supersymmetric standard model (MSSM), the gauge symmetry of the B-LSSM is extended by an additional  $U(1)_{B-L}$  gauge group, i.e. the full gauge structure is  $SU(3)_C \otimes SU(2)_L \otimes U(1)_Y \otimes U(1)_{B-L}$ . In addition to the MSSM superfields, two singlet chiral Higgs and three right-handed neutrinos with nonzero  $U(1)_{B-L}$  charge are introduced in the B-LSSM. The tiny neutrino masses can be acquired naturally through the so-called type I seesaw mechanism when the  $U(1)_{B-L}$  symmetry is broken spontaneously by the two newly introduced singlet Higgs. The mixings between the SM-like Higgs and the B-LSSM specific Higgs states are generated through the gauge kinetic mixing effect which arises in the NP models with two Abelian groups. It indicates that the

---

<sup>2</sup> Eq. (2) shows obviously that the ditau excess has large experimental uncertainties, combined with the analysis in Ref. [53] which indicates the CP-even dominated Higgs state has difficulties in describing the ditau excess, we focus on the diphoton and  $b\bar{b}$  excesses in this work.

rich Higgs sector and Higgs mixing effect provide great potential to explain the 95 GeV excesses. We take one of the B-LSSM specific CP-even Higgs states as the lightest Higgs to explore whether the B-LSSM can account for the low-mass diphoton and  $b\bar{b}$  excesses. It is known that the loop corrections from top and stop quarks are crucial to the SM-like Higgs boson mass in the supersymmetric models, the two-loop effective potential corrections from top and stop quarks to the CP-even neutral Higgs boson masses are considered in the calculations.

The paper is organized as follows. The scalar sector of the B-LSSM and the two-loop effective potential corrections to the CP-even neutral Higgs mass matrix are given in Sec. II. The numerical results are presented and analyzed in Sec. III. Finally, a summary is made in Sec. IV. The tedious formulae are collected in the appendix.

## II. THE B-LSSM AND HIGGS BOSON MASS WITH TWO-LOOP EFFECTIVE POTENTIAL CORRECTIONS

The gauge group of B-LSSM is extended by an additional  $U(1)_{B-L}$  local gauge group, and a new  $Z'$  gauge boson is introduced correspondingly. The chiral scalar superfields in the B-LSSM are

$$\begin{aligned}
H_d &= \begin{pmatrix} H_d^1 \\ H_d^2 \end{pmatrix} \sim (1, 2, -1/2, 0), \quad H_u = \begin{pmatrix} H_u^1 \\ H_u^2 \end{pmatrix} \sim (1, 2, 1/2, 0), \\
\eta &\sim (1, 1, 0, -1), \quad \bar{\eta} \sim (1, 1, 0, 1),
\end{aligned} \tag{5}$$

where the charges in the brackets correspond to  $SU(3)_C$ ,  $SU(2)_L$ ,  $U(1)_Y$ ,  $U(1)_{B-L}$  respectively. The local gauge symmetry  $SU(2)_L \otimes U(1)_Y \otimes U(1)_{B-L}$  breaks down to the electromagnetic symmetry  $U(1)_{em}$  as the Higgs fields receive nonzero vacuum expectation values (VEV):

$$\begin{aligned}
H_d^1 &= \frac{1}{\sqrt{2}}(v_d + \phi_d + i\sigma_d), & H_u^2 &= \frac{1}{\sqrt{2}}(v_u + \phi_u + i\sigma_u), \\
\eta &= \frac{1}{\sqrt{2}}(u_\eta + \phi_\eta + i\sigma_\eta), & \bar{\eta} &= \frac{1}{\sqrt{2}}(u_{\bar{\eta}} + \phi_{\bar{\eta}} + i\sigma_{\bar{\eta}}).
\end{aligned} \tag{6}$$



For convenience, we can define  $v^2 = v_d^2 + v_u^2$ ,  $u^2 = u_\eta^2 + u_{\bar{\eta}}^2$ ,  $\tan \beta = v_u/v_d$ ,  $\tan \beta' = u_{\bar{\eta}}/u_\eta$ .

The tree-level scalar potential in the B-LSSM can be written as [54]

$$\begin{aligned} V^{(0)} = & (m_{H_d}^2 + \mu^2)H_d^2 + (m_{H_u}^2 + \mu^2)H_u^2 + (m_\eta^2 + \mu_\eta^2)\eta^2 + (m_{\bar{\eta}}^2 + \mu_{\bar{\eta}}^2)\bar{\eta}^2 \\ & - 2B_\mu H_d H_u - 2B_\eta \eta \bar{\eta} + \frac{1}{8}(g_1^2 + g_2^2 + g_{YB}^2)(H_d^2 - H_u^2)^2 + \frac{1}{2}g_B^2(\eta^2 - \bar{\eta}^2)^2 \\ & + \frac{1}{2}g_B g_{YB}(H_d^2 - H_u^2)(\eta^2 - \bar{\eta}^2), \end{aligned} \quad (7)$$

where  $g_B$  is the gauge coupling constant corresponding to the  $U(1)_{B-L}$  gauge group,  $g_{YB}$  is the coupling constant arising from the kinetic mixing effect. For the one-loop and two-loop effective potential, the dominant contributions come from top and stop quarks. In the B-LSSM, the top quark mass reads

$$m_t = \frac{1}{\sqrt{2}}Y_t v_u. \quad (8)$$

The stop quark mass matrix can be written as

$$m_t^2 = \begin{pmatrix} m_{tL}^2, & \frac{Y_t}{\sqrt{2}}(v_u A_t - v_d \mu) \\ \frac{Y_t}{\sqrt{2}}(v_u A_t - v_d \mu), & m_{tR}^2 \end{pmatrix}, \quad (9)$$

where

$$\begin{aligned} m_{tL}^2 = & \frac{1}{24}[(g_1^2 - 3g_2^2 + g_{YB}^2 + g_B g_{YB})(v_u^2 - v_d^2) + 2g_B(g_B + g_{YB})(u_\eta^2 - u_{\bar{\eta}}^2)] \\ & + m_{\tilde{q}}^2 + \frac{1}{2}v_u^2 Y_t^2, \\ m_{tR}^2 = & \frac{1}{24}[(4g_1^2 + 4g_{YB}^2 + g_B g_{YB})(v_d^2 - v_u^2) + 2g_B(g_B + 4g_{YB})(u_\eta^2 - u_{\bar{\eta}}^2)] \\ & + m_{\tilde{u}}^2 + \frac{1}{2}v_u^2 Y_t^2. \end{aligned} \quad (10)$$

On the mass eigenstates, the physical stop masses can be written as

$$M_{t1,2}^2 = \frac{1}{2}(m_{tL}^2 + m_{tR}^2) \pm \left[ \frac{1}{4}(m_{tL}^2 - m_{tR}^2)^2 + \frac{1}{2}Y_t^2(v_u A_t - v_d \mu)^2 \right]^{1/2}. \quad (11)$$

The effective potential is

$$V_{\text{eff}} = V^{(0)} + \Delta V = V^{(0)} + V^{(1)} + V^{(2)}, \quad (12)$$

with [55–57]

$$\begin{aligned}
V^{(1)} &= -\frac{3}{16\pi^2}(m_t^2)^2(\log \frac{m_t^2}{Q^2} - \frac{3}{2}) + \frac{3}{32\pi^2} \sum_{i=1}^2 (M_{\tilde{t}_i}^2)^2 (\log \frac{M_{\tilde{t}_i}^2}{Q^2} - \frac{3}{2}), \\
V^{(2)} &= \frac{\alpha_s}{16\pi^3} \left\{ 2J(m_t^2, m_t^2) - 4m_t^2 I(m_t^2, m_t^2, 0) + \left[ 2M_{\tilde{t}_1}^2 I(M_{\tilde{t}_1}^2, M_{\tilde{t}_1}^2, 0) + 2L(M_{\tilde{t}_1}^2, M_{\tilde{g}}^2, m_t^2) \right. \right. \\
&\quad \left. \left. - 4m_t M_{\tilde{g}} S_{2\bar{\theta}} I(M_{\tilde{t}_1}^2, M_{\tilde{g}}^2, m_t^2) + \frac{1}{2}(1 + 2C_{2\bar{\theta}}^2)J(M_{\tilde{t}_1}^2, M_{\tilde{t}_1}^2) + \frac{S_{2\bar{\theta}}^2}{2}J(M_{\tilde{t}_1}^2, M_{\tilde{t}_2}^2) \right. \right. \\
&\quad \left. \left. + (M_{\tilde{t}_1} \leftrightarrow M_{\tilde{t}_2}, S_{2\bar{\theta}} \leftrightarrow -S_{2\bar{\theta}}) \right] \right\}, \tag{13}
\end{aligned}$$

where  $V^{(1)}$ ,  $V^{(2)}$  denote the one-loop and two-loop effective potential respectively. In Eq. (13),  $M_{\tilde{g}}$  is the mass of sgluon and

$$S_{2\bar{\theta}} = \frac{2(M_{\tilde{t}})_{12}}{M_{\tilde{t}_1}^2 - M_{\tilde{t}_2}^2}, \tag{14}$$

where  $(M_{\tilde{t}})_{12} = Y_t(v_u A_t - v_d \mu)$ . For the two-loop functions  $I$ ,  $J$  in Eq. (13) can be found in the appendix D of Ref. [58].

Combining Eq. (7) with Eq. (12), we can obtain the vacuum stability conditions

$$\begin{aligned}
m_{H_d}^2 + \mu^2 &= -\frac{\partial \Delta V}{v_d \partial \phi_d} - \frac{1}{4}g_B g_{YB}(v_\eta^2 - v_{\bar{\eta}}^2) + B_\mu \tan \beta - \frac{1}{8}(g_1^2 + g_2^2 + g_{YB}^2)(v_d^2 - v_u^2), \\
m_{H_u}^2 + \mu^2 &= -\frac{\partial \Delta V}{v_u \partial \phi_u} + \frac{1}{4}g_B g_{YB}(v_\eta^2 - v_{\bar{\eta}}^2) + B_\mu / \tan \beta + \frac{1}{8}(g_1^2 + g_2^2 + g_{YB}^2)(v_d^2 - v_u^2), \\
m_{H_\eta}^2 + \mu_\eta^2 &= -\frac{\partial \Delta V}{v_\eta \partial \phi_\eta} - \frac{1}{4}g_B g_{YB}(v_d^2 - v_u^2) + B_\eta \tan \beta' - \frac{1}{2}g_B^2(v_\eta^2 - v_{\bar{\eta}}^2), \\
m_{H_{\bar{\eta}}}^2 + \mu_{\bar{\eta}}^2 &= -\frac{\partial \Delta V}{v_{\bar{\eta}} \partial \phi_{\bar{\eta}}} + \frac{1}{4}g_B g_{YB}(v_d^2 - v_u^2) + B_{\bar{\eta}} / \tan \beta' + \frac{1}{2}g_B^2(v_\eta^2 - v_{\bar{\eta}}^2). \tag{15}
\end{aligned}$$

Then the elements of the CP-even Higgs squared mass matrix can be written as

$$\begin{aligned}
m_{\phi_d \phi_d}^2 &= \frac{1}{4}(g_1^2 + g_2^2 + g_{YB}^2)v_d^2 + B_\mu v_u / v_d + \left[ -\frac{1}{\phi_d} \frac{\partial \Delta V}{\partial \phi_d} + \frac{\partial^2 \Delta V}{\partial \phi_d \partial \phi_d} \right] \Big|_{\text{VEV}}, \\
m_{\phi_d \phi_u}^2 &= m_{\phi_u \phi_d}^2 = -B_\mu - \frac{1}{4}(g_1^2 + g_2^2 + g_{YB}^2)v_d v_u + \left[ \frac{\partial^2 \Delta V}{\partial \phi_d \partial \phi_u} \right] \Big|_{\text{VEV}}, \\
m_{\phi_d \phi_\eta}^2 &= m_{\phi_\eta \phi_d}^2 = \frac{1}{2}g_B g_{YB} v_d v_\eta + \left[ \frac{\partial^2 \Delta V}{\partial \phi_d \partial \phi_\eta} \right] \Big|_{\text{VEV}}, \\
m_{\phi_d \phi_{\bar{\eta}}}^2 &= m_{\phi_{\bar{\eta}} \phi_d}^2 = -\frac{1}{2}g_B g_{YB} v_d v_{\bar{\eta}} + \left[ \frac{\partial^2 \Delta V}{\partial \phi_d \partial \phi_{\bar{\eta}}} \right] \Big|_{\text{VEV}}, \\
m_{\phi_u \phi_u}^2 &= \frac{1}{4}(g_1^2 + g_2^2 + g_{YB}^2)v_u^2 + B_\mu v_d / v_u + \left[ -\frac{1}{\phi_u} \frac{\partial \Delta V}{\partial \phi_u} + \frac{\partial^2 \Delta V}{\partial \phi_u \partial \phi_u} \right] \Big|_{\text{VEV}},
\end{aligned}$$

$$\begin{aligned}
m_{\phi_u\phi_\eta}^2 &= m_{\phi_\eta\phi_u}^2 = -\frac{1}{2}g_B g_Y B v_u v_\eta + \left[ \frac{\partial^2 \Delta V}{\partial \phi_u \partial \phi_\eta} \right] \Big|_{\text{VEV}}, \\
m_{\phi_u\phi_{\bar{\eta}}}^2 &= m_{\phi_{\bar{\eta}}\phi_u}^2 = \frac{1}{2}g_B g_Y B v_u v_{\bar{\eta}} + \left[ \frac{\partial^2 \Delta V}{\partial \phi_u \partial \phi_{\bar{\eta}}} \right] \Big|_{\text{VEV}}, \\
m_{\phi_\eta\phi_\eta}^2 &= g_B^2 v_\eta^2 + B_\eta v_{\bar{\eta}}/v_\eta + \left[ -\frac{1}{\phi_\eta} \frac{\partial \Delta V}{\partial \phi_\eta} + \frac{\partial^2 \Delta V}{\partial \phi_\eta \partial \phi_\eta} \right] \Big|_{\text{VEV}}, \\
m_{\phi_\eta\phi_{\bar{\eta}}}^2 &= m_{\phi_{\bar{\eta}}\phi_\eta}^2 = -B_\eta - g_B^2 v_\eta v_{\bar{\eta}} + \left[ \frac{\partial^2 \Delta V}{\partial \phi_\eta \partial \phi_{\bar{\eta}}} \right] \Big|_{\text{VEV}}, \\
m_{\phi_{\bar{\eta}}\phi_{\bar{\eta}}}^2 &= g_B^2 v_{\bar{\eta}}^2 + B_\eta v_\eta/v_{\bar{\eta}} + \left[ -\frac{1}{\phi_{\bar{\eta}}} \frac{\partial \Delta V}{\partial \phi_{\bar{\eta}}} + \frac{\partial^2 \Delta V}{\partial \phi_{\bar{\eta}} \partial \phi_{\bar{\eta}}} \right] \Big|_{\text{VEV}},
\end{aligned} \tag{16}$$

where the detailed calculations of the contributions from  $\Delta V$  in Eq. (16) are collected in the appendix. The tree-level squared Higgs mass matrix in the B-LSSM can be read easily in Eq. (16). And to illustrate clearly that the rich Higgs sector in the B-LSSM provides the potential to explain the 95 GeV excesses, we calculate the eigenvalues of the tree-level squared Higgs mass matrix under the approximation  $v^2 \ll u^2$ , the analytical results can be written as

$$\begin{aligned}
m_{h_{1,\text{tree}}}^2 &\approx \frac{2B_\eta(\tan^2 \beta' - 1)^2}{1 + (\tan^2 \beta' + 1)B_\eta/(g_B^2 u^2)}, & m_{h_{2,\text{tree}}}^2 &\approx \frac{(g_1^2 + g_2^2 + g_{YB}^2)(\tan^2 \beta - 1)^2 v^2}{4(\tan^2 \beta + 1)^2}, \\
m_{h_{3,\text{tree}}}^2 &\approx \frac{B_\mu}{\tan \beta}(\tan^2 \beta + 1), & m_{h_{4,\text{tree}}}^2 &\approx 2\left(\frac{g_B^2 u^2}{\tan^2 \beta + 1} + B_\eta\right),
\end{aligned} \tag{17}$$

where the terms proportional to  $\mathcal{O}[(\tan^2 \beta' - 1)^3]$  are neglected for simplicity,  $m_{h_i,\text{tree}} < m_{h_j,\text{tree}}$  for  $i < j$ , and  $m_{h_{1,\text{tree}}}$ ,  $m_{h_{4,\text{tree}}}$  are the tree-level masses of the states dominated by the two specific scalar singlets in the B-LSSM,  $m_{h_{2,\text{tree}}}$ ,  $m_{h_{3,\text{tree}}}$  are the tree-level masses of the states dominated by the two scalar doublets which correspond to the two scalar doublets in the MSSM. As shown in Eq. (17),  $m_{h_{2,\text{tree}}}$  corresponds to the mass of SM-like Higgs, and  $m_{h_{3,\text{tree}}} \approx m_A \gtrsim 380$  GeV [59] with  $m_A$  denoting the CP-odd Higgs mass in the MSSM, which also indicates the 95 GeV Higgs can not be achieved in the MSSM. However, the expression of  $m_{h_{1,\text{tree}}}$  in Eq. (17) shows that the 95 GeV Higgs can be obtained in the B-LSSM when  $\tan \beta' - 1$  approaches to 0 or  $B_\eta$  is small. Combined with the tree-level mixing with the SM-like Higgs as presented in Eq. (16), the B-LSSM has great potential to explain the observed 95 GeV excesses, while the excesses can not be explained in the frame work of MSSM [60].

On the basis  $(\phi_d, \phi_u, \phi_\eta, \phi_{\bar{\eta}})$ , the squared mass matrix of CP-even Higgs can be written as

$$M_\phi^2 = \begin{pmatrix} m_{\phi_d\phi_d}^2 & m_{\phi_d\phi_u}^2 & m_{\phi_d\phi_\eta}^2 & m_{\phi_d\phi_{\bar{\eta}}}^2 \\ m_{\phi_d\phi_u}^2 & m_{\phi_u\phi_u}^2 & m_{\phi_u\phi_\eta}^2 & m_{\phi_u\phi_{\bar{\eta}}}^2 \\ m_{\phi_d\phi_\eta}^2 & m_{\phi_u\phi_\eta}^2 & m_{\phi_\eta\phi_\eta}^2 & m_{\phi_\eta\phi_{\bar{\eta}}}^2 \\ m_{\phi_d\phi_{\bar{\eta}}}^2 & m_{\phi_u\phi_{\bar{\eta}}}^2 & m_{\phi_\eta\phi_{\bar{\eta}}}^2 & m_{\phi_{\bar{\eta}}\phi_{\bar{\eta}}}^2 \end{pmatrix}. \quad (18)$$

In order to present the mass matrices of the Higgs fields in a physical way, we rotate the fields  $H_d, H_u, \eta, \bar{\eta}$  as

$$\begin{aligned} H_1 &= \cos \beta H_u + \sin \beta H_d, & H_2 &= \cos \beta H_d - \sin \beta H_u, \\ H_3 &= \cos \beta' \bar{\eta} + \sin \beta' \eta, & H_4 &= \cos \beta' \eta - \sin \beta' \bar{\eta}, \end{aligned} \quad (19)$$

where  $H_2$  corresponds to the SM Higgs doublet [25]. Then on the basis  $(\phi_1, \phi_2, \phi_3, \phi_4)$ , the squared mass matrix of CP-even Higgs can be written as

$$M_h^2 = U \cdot M_\phi^2 \cdot U^\dagger, \quad (20)$$

where

$$U = \begin{pmatrix} \sin \beta & \cos \beta & 0 & 0 \\ \cos \beta & -\sin \beta & 0 & 0 \\ 0 & 0 & \sin \beta' & \cos \beta' \\ 0 & 0 & \cos \beta' & -\sin \beta' \end{pmatrix}, \quad (21)$$

$$\begin{aligned} \phi_1 &= \cos \beta \phi_u + \sin \beta \phi_d, & \phi_2 &= \cos \beta \phi_d - \sin \beta \phi_u, \\ \phi_3 &= \cos \beta' \phi_{\bar{\eta}} + \sin \beta' \phi_\eta, & \phi_4 &= \cos \beta' \phi_\eta - \sin \beta' \phi_{\bar{\eta}}. \end{aligned} \quad (22)$$

The squared mass matrix  $M_h^2$  can be diagonalized by the unitary matrix  $Z_h$  as

$$\text{diag}(m_{h_1}^2, m_{h_2}^2, m_{h_3}^2, m_{h_4}^2) = Z_h \cdot M_h^2 \cdot Z_h^\dagger, \quad (23)$$

where  $h_i, (i = 1, 2, 3, 4)$  denote the mass eigenstates.

As defined in the introduction sector, the diphoton and  $b\bar{b}$  signal strength are

$$\begin{aligned}\mu(h_{95})_{\gamma\gamma} &= \frac{\sigma(gg \rightarrow h_{95}^{\text{NP}})\text{BR}(h_{95}^{\text{NP}} \rightarrow \gamma\gamma)}{\sigma(gg \rightarrow h_{95}^{\text{SM}})\text{BR}(h_{95}^{\text{SM}} \rightarrow \gamma\gamma)}, \\ \mu(h_{95})_{b\bar{b}} &= \frac{\sigma(Z^* \rightarrow Zh_{95}^{\text{NP}})\text{BR}(h_{95}^{\text{NP}} \rightarrow b\bar{b})}{\sigma(Z^* \rightarrow Zh_{95}^{\text{SM}})\text{BR}(h_{95}^{\text{SM}} \rightarrow b\bar{b})},\end{aligned}\quad (24)$$

where [61]

$$\begin{aligned}\Gamma_{\text{tot}}^{\text{SM}} &\approx 0.0026 \text{ GeV}, \\ \text{BR}(h_{95}^{\text{SM}} \rightarrow \gamma\gamma) &\approx 1.4 \times 10^{-3}, \quad \text{BR}(h_{95}^{\text{SM}} \rightarrow b\bar{b}) \approx 0.81.\end{aligned}\quad (25)$$

Since top quark makes the dominant contributions to the Higgs production, the cross section for  $gg \rightarrow h_{95}^{\text{NP}}$  and  $\sigma(Z^* \rightarrow Zh_{95}^{\text{NP}})$  can be estimated by [25]

$$\begin{aligned}\sigma(gg \rightarrow h_{95}^{\text{NP}}) &\approx C_{h_{95}uu}^2 \sigma(gg \rightarrow h_{95}^{\text{SM}}), \\ \sigma(Z^* \rightarrow Zh_{95}^{\text{NP}}) &\approx C_{h_{95}VV}^2 \sigma(Z^* \rightarrow Zh_{95}^{\text{SM}}),\end{aligned}\quad (26)$$

where the coefficients  $C_{h_{95}uu}$ ,  $C_{h_{95}VV}$  are the normalized couplings of 95 GeV Higgs in NP models with up-quarks and gauge bosons respectively (in units of the corresponding SM couplings). The branch ratios for  $h_{95}^{\text{NP}} \rightarrow \gamma\gamma$  or  $b\bar{b}$  can be estimated by [25]

$$\begin{aligned}\text{BR}(h_{95}^{\text{NP}} \rightarrow \gamma\gamma) &\approx C_{h_{95}uu}^2 \text{BR}(h_{95}^{\text{SM}} \rightarrow \gamma\gamma) \frac{\Gamma_{\text{tot}}^{\text{SM}}}{\Gamma_{\text{tot}}^{\text{NP}}}, \\ \text{BR}(h_{95}^{\text{NP}} \rightarrow b\bar{b}) &\approx C_{h_{95}dd}^2 \text{BR}(h_{95}^{\text{SM}} \rightarrow b\bar{b}) \frac{\Gamma_{\text{tot}}^{\text{SM}}}{\Gamma_{\text{tot}}^{\text{NP}}},\end{aligned}\quad (27)$$

where the coefficients  $C_{h_{95}dd}$  is the normalized couplings of 95 GeV Higgs in NP models with down-quarks, and [61]

$$\begin{aligned}\Gamma_{\text{tot}}^{\text{NP}} &\approx C_{h_{95}dd}^2 (\Gamma_{b\bar{b}}^{\text{SM}} + \Gamma_{\tau\bar{\tau}}^{\text{SM}}) + C_{h_{95}uu}^2 (\Gamma_{c\bar{c}}^{\text{SM}} + \Gamma_{gg}^{\text{SM}}) + C_{h_{95}VV}^2 \Gamma_{WW^*}^{\text{SM}}, \\ \text{BR}(h_{95}^{\text{SM}} \rightarrow \tau\tau) &\approx 0.082, \quad \text{BR}(h_{95}^{\text{SM}} \rightarrow c\bar{c}) \approx 0.037, \quad \text{BR}(h_{95}^{\text{SM}} \rightarrow gg) \approx 0.058, \\ \text{BR}(h_{95}^{\text{SM}} \rightarrow WW^*) &\approx 0.012.\end{aligned}\quad (28)$$

In the B-LSSM, we have

$$\begin{aligned}C_{h_{95}uu} = C_{h_{11}uu} &= Z_{h,11} \cot \beta + Z_{h,12}, \quad C_{h_{95}dd} = C_{h_{11}dd} = Z_{h,11} \tan \beta + Z_{h,12}, \\ C_{h_{95}VV} = C_{h_{11}VV} &= Z_{h,12}.\end{aligned}\quad (29)$$

### III. NUMERICAL RESULTS

Taking the lightest Higgs mass at around 95 GeV and the next-to-lightest Higgs mass at the measured SM-like Higgs mass [59]

$$m_h = 125.09 \pm 0.24 \text{ GeV}, \quad (30)$$

we present the numerical results of the two light Higgs masses, the diphoton and  $b\bar{b}$  signal strengths in this section.

To carry out the numerical evaluations, we take the relevant SM input parameters as  $m_W = 80.385$  GeV,  $m_Z = 90.1876$  GeV,  $\alpha_{em}(m_Z) = 1/128.9$ ,  $\alpha_s(m_Z) = 0.118$ . Due to the introducing of  $U(1)_{B-L}$  gauge group, a new  $Z'$  gauge boson is introduced in the B-LSSM. Refs. [62–64] give an upper bound on the ratio between the  $Z'$  mass  $M_{Z'} \approx \frac{1}{2}g_B u$  and its gauge coupling at 99% CL as

$$M_{Z'}/g_B \geq 6 \text{ TeV}. \quad (31)$$

For simplicity, we take  $g_B = 0.5$  in the following analysis, and Eq. (31) indicates  $M_{Z'} \geq 3$  TeV in this case. As analyzed in Refs. [65, 66], the effects of new  $Z'$  in the B-LSSM on the couplings of  $Z$ -charged leptons which are measured at LEP precisely [59], can be eliminated by redefining the neutral currents involving charged leptons. It indicates that the redefined  $Z$  boson in the B-LSSM can coincide with the one measured at the LEP [59]. The LHC experimental data constrains  $\tan \beta' < 1.5$  [67]. Based on the analysis about  $\bar{B} \rightarrow X_s \gamma$  and  $B_s^0 \rightarrow \mu^+ \mu^-$  in our previous work [68], we take  $m_{H^\pm} = 1.5$  TeV. To coincide with the constraints from the direct searches of squarks, sgluon at the LHC [69, 70] and the observed Higgs signal analyzed in Ref. [71], we take  $m_{\tilde{g}} = m_{\tilde{q}} = m_{\tilde{u}} = 2.5$  TeV for simplicity. It is well known that squarks can make contributions at the one-loop level to the oblique parameters  $S$ ,  $T$ ,  $U$ , which suffer strict constraints from the LEP measurements [59]. Hence, the contributions from squarks in the B-LSSM to  $S$ ,  $T$ ,  $U$  parameters are calculated and the details are collected in the appendix B. We verify numerically that the  $S$ ,  $T$ ,  $U$  parameters can satisfy the LEP measurements for the chosen squark masses.

Firstly, we investigate the masses of the lightest and next-to-lightest Higgs bosons within the B-LSSM. Taking  $g_{YB} = -0.4$ ,  $M_{Z'} = 4.2$  TeV,  $B_\eta = (1 \text{ TeV})^2$ , we plot  $m_{h_i}$  versus  $\tan \beta'$

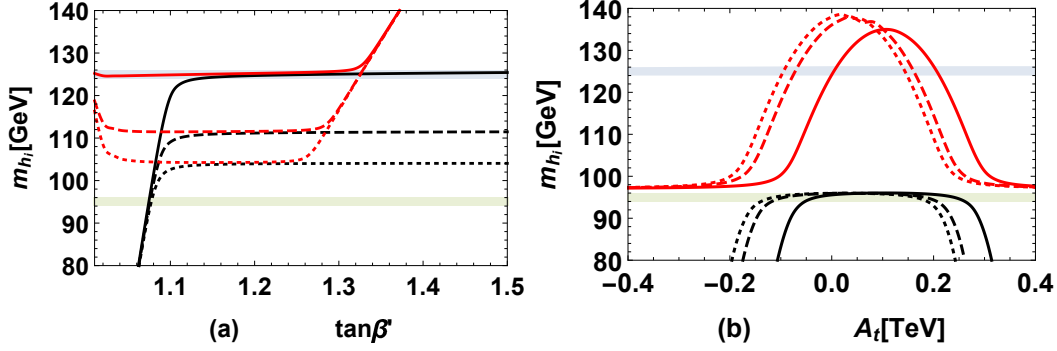


FIG. 1: Taking  $g_{YB} = -0.4$ ,  $M_{Z'} = 4.2$  TeV,  $B_\eta = (1 \text{ TeV})^2$ ,  $m_{h_i}$  versus  $\tan \beta'$  for  $A_t = 0.2$  TeV is plotted in (a), and  $m_{h_i}$  versus  $A_t$  for  $\tan \beta' = 1.075$  is plotted in (b). The black, red lines denote the results for  $m_{h_1}$ ,  $m_{h_2}$  respectively, the solid, dashed, dotted lines denote the results for  $\tan \beta = 5, 15, 25$  respectively, the green areas denote the range  $94 \text{ GeV} < m_{h_i} < 96 \text{ GeV}$ , the gray areas denote the range  $124 \text{ GeV} < m_{h_i} < 126 \text{ GeV}$ .

for  $A_t = 0.2$  TeV in Fig. 1 (a), and  $m_{h_i}$  versus  $A_t$  for  $\tan \beta' = 1.075$  in Fig. 1 (b). Where the black, red lines denote the results for  $m_{h_1}$ ,  $m_{h_2}$  respectively, the solid, dashed, dotted lines denote the results for  $\tan \beta = 5, 15, 25$  respectively, the green areas denote the range  $94 \text{ GeV} < m_{h_i} < 96 \text{ GeV}$ , the gray areas denote the range  $124 \text{ GeV} < m_{h_i} < 126 \text{ GeV}$ . It can be noted from the picture that  $\tan \beta'$ ,  $\tan \beta$  and  $A_t$  affect the two light Higgs boson masses obviously. Importantly, both the 95 GeV Higgs and the SM-like Higgs with a mass of 125 GeV are attainable within the B-LSSM. Fig. 1 (a) demonstrates that  $\tan \beta'$  is constrained strictly for  $m_{h_1} \approx 95$  GeV in our chosen parameter space, and the effects of  $\tan \beta'$  on  $m_{h_i}$  ( $i = 1, 2$ ) are influenced significantly by the value of  $\tan \beta$ . This fact can be seen explicitly in Eq. (17). From Fig. 1 (b) we can see that  $A_t$  is subject to a strict limitation through the requirement of setting  $m_{h_2} \approx 125$  GeV.

As shown in Eq. (17), the lightest Higgs boson is dominated by one of the B-LSSM specific Higgs states, and  $B_\eta$ ,  $g_{YB}$ ,  $M_{Z'}$  can affect the theoretical predictions on the two light Higgs boson masses significantly. Then we take  $\tan \beta' = 1.075$ ,  $\tan \beta = 5$ ,  $A_t = 0.2$  TeV and plot  $m_{h_i}$  versus  $B_\eta$  for  $M_{Z'} = 4.2$  TeV in Fig. 2 (a), and  $m_{h_i}$  versus  $M_{Z'}$  for  $B_\eta = (1 \text{ TeV})^2$  in Fig. 2 (b). Where the black, red lines denote the results for  $m_{h_1}$ ,  $m_{h_2}$  respectively, the

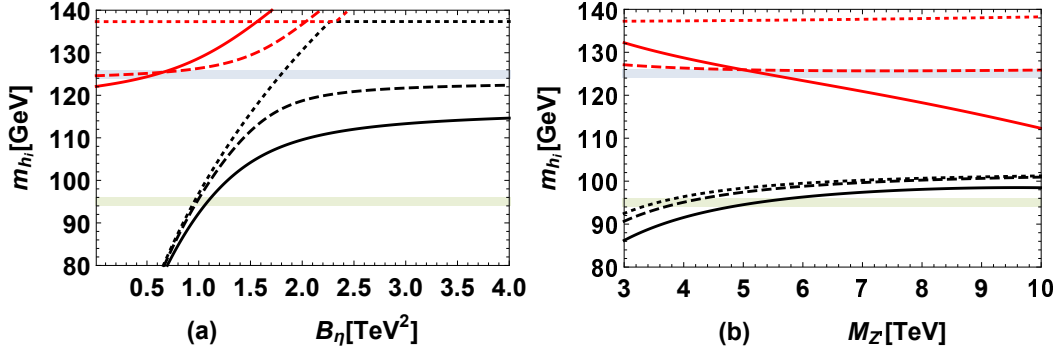


FIG. 2: Taking  $\tan \beta' = 1.075$ ,  $\tan \beta = 5$ ,  $A_t = 0.2$  TeV,  $m_{h_i}$  versus  $B_\eta$  for  $M_{Z'} = 4.2$  TeV is plotted in (a), and  $m_{h_i}$  versus  $M_{Z'}$  for  $B_\eta = (1 \text{ TeV})^2$  is plotted in (b). The black, red lines denote the results for  $m_{h_1}$ ,  $m_{h_2}$  respectively, the solid, dashed, dotted lines denote the results for  $g_{YB} = -0.8, -0.4, 0$  respectively, the green areas denote the range  $94 \text{ GeV} < m_{h_i} < 96 \text{ GeV}$ , the gray areas denote the range  $124 \text{ GeV} < m_{h_i} < 126 \text{ GeV}$ .

solid, dashed, dotted lines denote the results for  $g_{YB} = -0.8, -0.4, 0$  respectively, the green areas denote the range  $94 \text{ GeV} < m_{h_i} < 96 \text{ GeV}$ , the gray areas denote the range  $124 \text{ GeV} < m_{h_i} < 126 \text{ GeV}$ .

Fig. 2 (a) shows that both  $m_{h_1}$  and  $m_{h_2}$  increase as  $B_\eta$  increases, and the dotted lines intersect. At  $g_{YB} = 0$ , there is no mixing effects between the SM-like Higgs with the B-LSSM specific Higgs states at the tree level (the fact can be seen obviously in Eq. (16)). In this scenario,  $h_2$  is primarily governed by the SM-like Higgs state and  $m_{h_2}$  does not depend on the value of  $B_\eta$ . Conversely,  $m_{h_1}$  is dominated by the B-LSSM specific Higgs state and rises with increasing  $B_\eta$ . As  $B_\eta$  increases, the mass of the B-LSSM specific Higgs state surpasses the mass of the SM-like Higgs state, causing  $h_1$  to be dominated by the SM-like Higgs state and  $h_2$  to be dominated by the B-LSSM specific Higgs state. This situation results in the intersection of the two dotted lines in Fig. 2 (a). The three red lines in Fig. 2 (b) show that  $M_{Z'}$  affects  $m_{h_2}$  obviously when  $g_{YB} = -0.8$ , because the mixing effects between the SM-like Higgs with the B-LSSM specific Higgs states are large for large  $g_{YB}$  and play important roles on SM-like Higgs boson masses.

Based on the preceding analysis, it is evident that both the 95 GeV Higgs boson and the



125 GeV SM-like Higgs boson are attainable in the B-LSSM. Due to the masses of the two light Higgs bosons are influenced significantly in a complex manner by  $\tan \beta$ ,  $\tan \beta'$ ,  $A_t$ ,  $B_\eta$ ,  $g_{YB}$ ,  $M_{Z'}$ , we scan the following parameter space

$$\begin{aligned} \tan \beta &= (2, 40), \quad \tan \beta' = (1, 1.5), \quad A_t = (-1, 1) \text{ TeV}, \\ B_\eta &= (0.1^2, 2^2) \text{ TeV}^2, \quad g_{YB} = (-1, 0), \quad M_{Z'} = (3, 10) \text{ TeV}, \end{aligned} \quad (32)$$

to comprehensively explore the collective influences of  $\tan \beta$ ,  $\tan \beta'$ ,  $A_t$ ,  $B_\eta$ ,  $g_{YB}$ ,  $M_{Z'}$  on the signal strengthes of diphoton and  $b\bar{b}$  events, and keep  $94 \text{ GeV} < m_{h_1} < 96 \text{ GeV}$ ,  $124 \text{ GeV} < m_{h_2} < 126 \text{ GeV}$  in the scanning. It can be noted in Eq. (32) that we take  $\tan \beta$  in the range  $2 < \tan \beta < 40$ , and the neutral and charged Higgs are limited to be heavier for larger  $\tan \beta$  by the LHC searches [59]. For  $\tan \beta = 40$ , the neutral Higgs mass and charged Higgs mass are required to be larger than about 1.3 TeV, 0.9 TeV respectively [59]. In our chosen parameter space, the charged Higgs mass is taken as  $m_{H^\pm} = 1.5 \text{ TeV}$  for simplicity as mentioned above, and the two neutral Higgs masses are larger than 1.4 TeV, which indicate that the chosen parameter space well coincide with the LHC searches.

To explore the best fit describing 125 GeV Higgs mass and the diphoton,  $b\bar{b}$  excesses, a  $\chi^2$  test is performed. The  $\chi^2$  function can be constructed as

$$\chi^2 = \sum_1 \left( \frac{O_i^{\text{th}} - O_i^{\text{exp}}}{\sigma_i^{\text{exp}}} \right)^2, \quad (33)$$

where  $O_i^{\text{th}}$  denotes the  $i$ -th observable computed theoretically,  $O_i^{\text{exp}}$  is the corresponding experimental value and  $\sigma_i^{\text{exp}}$  is the uncertainty in  $O_i^{\text{exp}}$ . Then the allowed ranges of  $A_t - \tan \beta$ ,  $B_\eta - \tan \beta'$ ,  $M_{Z'} - g_{YB}$  are plotted in Fig. 3 (a), Fig. 3 (b), Fig. 3 (c) respectively, and the obtained  $\mu(h_{95})_{\gamma\gamma} - \mu(h_{95})_{bb}$  is plotted in Fig. 3 (d). In Fig. 3, the ‘black stars’ denote the best fit corresponding to  $\chi^2 = 0.058$  with the diphoton excess in Eq. (3),  $b\bar{b}$  excess in Eq. (4) and 125 GeV Higgs mass in Eq. (30), the gray points denote the results excluded by considering the  $\mu(h_{95})_{\gamma\gamma}$ ,  $\mu(h_{95})_{bb}$  in the experimental  $2\sigma$  intervals, and the green points, orange points denote the results with  $\mu(h_{95})_{\gamma\gamma}$ ,  $\mu(h_{95})_{bb}$  in the experimental  $1\sigma$ ,  $2\sigma$  intervals respectively.

The green points in Fig. 3 indicates obviously that the B-LSSM can reproduce the diphoton and  $b\bar{b}$  excesses in the experimental  $1\sigma$  intervals simultaneously. Fig. 3 (a) shows that

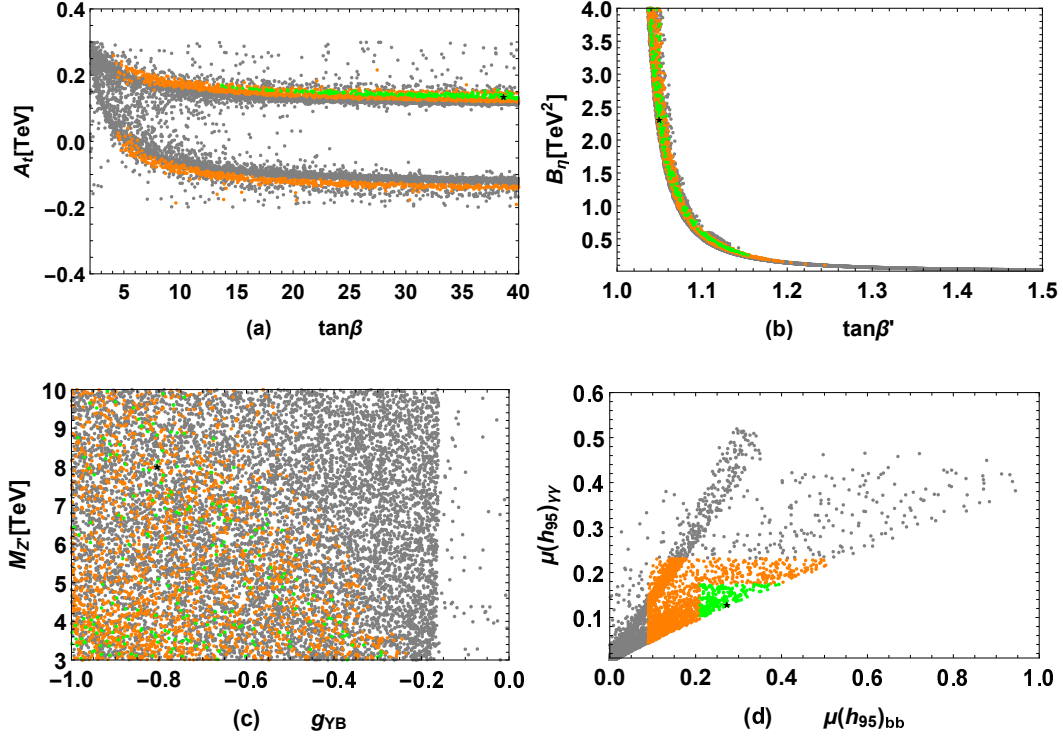


FIG. 3: Scanning the parameter space in Eq. (32) and keeping  $94 \text{ GeV} < m_{h_1} < 96 \text{ GeV}$ ,  $124 \text{ GeV} < m_{h_2} < 126 \text{ GeV}$  in the scanning, the allowed ranges of  $A_t - \tan\beta$  (a),  $B_\eta - \tan\beta'$  (b),  $M_{Z'} - g_{YB}$  (c) and the obtained  $\mu(h_{95})_{\gamma\gamma} - \mu(h_{95})_{bb}$  (d) are plotted. The ‘black stars’ denote the best fit corresponding to  $\chi^2 = 0.058$  with the diphoton excess in Eq. (3),  $b\bar{b}$  excess in Eq. (4) and 125 GeV Higgs mass in Eq. (30), the gray points denote the results excluded by considering the  $\mu(h_{95})_{\gamma\gamma}$ ,  $\mu(h_{95})_{bb}$  in the experimental  $2\sigma$  intervals, and the green, orange points denote the results with  $\mu(h_{95})_{\gamma\gamma}$ ,  $\mu(h_{95})_{bb}$  in the experimental  $1\sigma$ ,  $2\sigma$  intervals respectively.

negative  $A_t$  is excluded by considering the two excesses in the experimental  $1\sigma$  interval, while the negative  $A_t$  is allowed for the case of considering the experimental  $2\sigma$  interval, and most of  $A_t$  are excluded by the conditions  $94 \text{ GeV} < m_{h_1} < 96 \text{ GeV}$ ,  $124 \text{ GeV} < m_{h_2} < 126 \text{ GeV}$ . As shown in Fig. 3 (b), the two light Higgs masses prefer large  $B_\eta$  for small  $\tan\beta'$  and  $B_\eta$  is limited strictly for given  $\tan\beta'$ , because  $B_\eta$ ,  $\tan\beta'$  affect the two light Higgs boson mass significantly as shown in Eq. (17). In addition,  $\tan\beta'$  is limited in the range  $1.04 \lesssim \tan\beta' \lesssim 1.16$

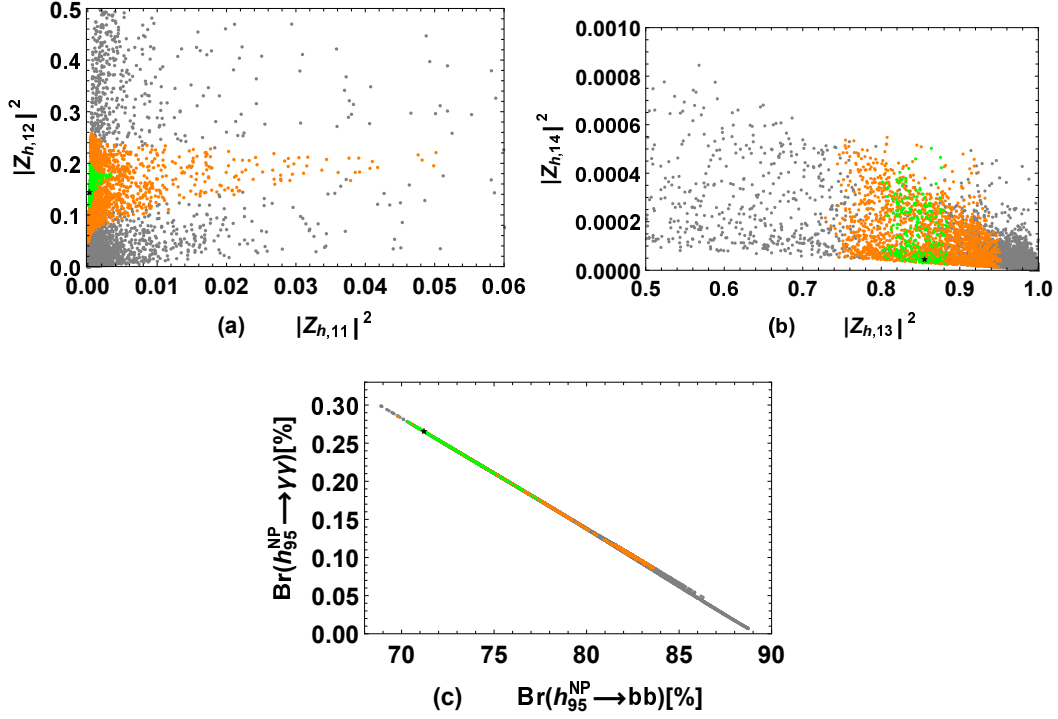


FIG. 4: Scanning the parameter space in Eq. (32) and keeping  $94 \text{ GeV} < m_{h_1} < 96 \text{ GeV}$ ,  $124 \text{ GeV} < m_{h_2} < 126 \text{ GeV}$  in the scanning, the results of  $|Z_{h,11}|^2 - |Z_{h,12}|^2$  (a),  $|Z_{h,13}|^2 - |Z_{h,14}|^2$  (b) and  $\text{Br}(h_{95}^{\text{NP}} \rightarrow \gamma\gamma) - \text{Br}(h_{95}^{\text{NP}} \rightarrow b\bar{b})$  (c) are plotted, where the ‘black stars’ denote the best fit corresponding to  $\chi^2 = 0.058$  with the diphoton excess in Eq. (3),  $b\bar{b}$  excess in Eq. (4) and 125 GeV Higgs mass in Eq. (30), the gray points denote the results excluded by considering the two excesses in the experimental  $2\sigma$  intervals, and the green, orange points denote the results with  $\mu(h_{95})_{\gamma\gamma}$ ,  $\mu(h_{95})_{b\bar{b}}$  in the experimental  $1\sigma$ ,  $2\sigma$  intervals respectively.

by considering the two excesses in the experimental  $1\sigma$  interval. Fig. 3 (c) shows that  $g_{YB}$  is limited in the range  $g_{YB} \lesssim -0.3$  and  $M_{Z'}/|g_{YB}| \lesssim 11 \text{ TeV}$  by considering the two excesses in the experimental  $1\sigma$  interval, which provides a new bound on the ratio of  $Z'$  boson mass with the kinetic mixing parameter  $g_{YB}$  if the diphoton and  $b\bar{b}$  excesses are verified in future.

Finally, in order to show explicitly the components of the lightest 95 GeV Higgs and the results of  $\text{Br}(h_{95}^{\text{NP}} \rightarrow \gamma\gamma)$ ,  $\text{Br}(h_{95}^{\text{NP}} \rightarrow b\bar{b})$  analyzed in Fig. 3, we present the results of  $|Z_{h,11}|^2 - |Z_{h,12}|^2$ ,  $|Z_{h,13}|^2 - |Z_{h,14}|^2$ ,  $\text{Br}(h_{95}^{\text{NP}} \rightarrow \gamma\gamma) - \text{Br}(h_{95}^{\text{NP}} \rightarrow b\bar{b})$  in Fig. 4 (a), Fig. 4 (b),

Fig. 4 (c) respectively. The definitions of the ‘black stars’, gray points, green points, orange points are same to the ones of Fig. 3. It is obvious in Fig. 4 (a), (b) that the lightest 95 GeV Higgs is dominated by the new scalar singlets introduced in the B-LSSM, and the mixing effects between scalar doublets with B-LSSM specific scalar singlets provide the potential to explain diphoton and  $b\bar{b}$  excesses at about 95 GeV. It indicates that considering the two loop effective potential corrections is valuable in calculating the two light Higgs boson masses and the scalar mixing effects. In addition, Fig. 4 (c) shows that considering  $\mu(h_{95})_{\gamma\gamma}$ ,  $\mu(h_{95})_{bb}$  in the experimental  $2\sigma$  intervals prefers  $\text{Br}(h_{95}^{\text{NP}} \rightarrow \gamma\gamma)$  and  $\text{Br}(h_{95}^{\text{NP}} \rightarrow bb)$  in the ranges  $(0.17 \sim 0.28)\%$  and  $(70.3 \sim 77.5)\%$  respectively, which are different from the corresponding branching ratios of  $h_{95}^{\text{SM}}$ .

#### IV. SUMMARY

Motivated by the diphoton and  $b\bar{b}$  excesses at a mass about 95 GeV in the CMS and LEP data, and the B-LSSM can produce a 95 GeV light Higgs naturally due to the introducing of two specific singlet states, our investigation is centered on the analysis of the two light Higgs boson masses along with the corresponding diphoton and  $b\bar{b}$  signal strengths within the B-LSSM framework. The two loop effective potential corrections to the squared Higgs mass matrix are considered in the calculations, because the loop corrections play crucial roles in determining the SM-like Higgs boson mass within the supersymmetric models. Considering the lightest Higgs boson mass at about 95 GeV and the next-to-lightest Higgs boson mass at about 125 GeV, it is found that the B-LSSM specific Higgs states can account for the observed diphoton and  $b\bar{b}$  excesses around 95 GeV simultaneously. As we consider the B-LSSM specific Higgs state as the lightest Higgs boson, the specific parameters  $\tan\beta'$ ,  $B_\eta$ ,  $g_{YB}$  and  $M_{Z'}$  in the B-LSSM affect the theoretical predictions on the two light Higgs boson masses significantly. Fitting  $\mu(h_{95})_{\gamma\gamma}$ ,  $\mu(h_{95})_{bb}$  in the experimental  $1\sigma$  interval will impose stringent constraints on the parameter space of the B-LSSM, and a new bound on the ratio of  $Z'$  boson mass with the kinetic mixing parameter  $g_{YB}$  can be provided if the diphoton and  $b\bar{b}$  excesses at about 95 GeV are verified in future. In addition, considering the two loop effective potential corrections is valuable in calculating the two light Higgs boson masses

and the scalar mixing effects, which play important roles in explaining the excesses at about 95 GeV.

### Appendix A: The two-loop effective potential corrections to the CP-even neutral Higgs mass matrix.

Generally, the corrections from the effective potential  $\Delta V$  to the CP-even neutral Higgs boson masses can be written as

$$\begin{aligned}
\left[ -\frac{1}{\phi_d} \frac{\partial \Delta V}{\partial \phi_d} + \frac{\partial^2 \Delta V}{\partial \phi_d \partial \phi_d} \right] \Big|_{VEV} &= -\frac{1}{v_d} \left[ \frac{\partial \Delta V}{\partial M_{t_1}^2} \frac{\partial M_{t_1}^2}{\partial \phi_d} + \frac{\partial \Delta V}{\partial M_{t_2}^2} \frac{\partial M_{t_2}^2}{\partial \phi_d} + \frac{\partial \Delta V}{\partial C_{2\theta_t}^2} \frac{\partial C_{2\theta_t}^2}{\partial \phi_d} \right] \\
&+ \frac{\partial^2 \Delta V}{\partial M_{t_1}^2 \partial M_{t_1}^2} \left( \frac{\partial M_{t_1}^2}{\partial \phi_d} \right)^2 + \frac{\partial \Delta V}{\partial M_{t_1}^2} \frac{\partial^2 M_{t_1}^2}{\partial \phi_d \partial \phi_d} + 2 \frac{\partial^2 \Delta V}{\partial M_{t_1}^2 \partial M_{t_2}^2} \frac{\partial M_{t_1}^2}{\partial \phi_d} \frac{\partial M_{t_2}^2}{\partial \phi_d} \\
&+ \frac{\partial^2 \Delta V}{\partial M_{t_2}^2 \partial M_{t_2}^2} \left( \frac{\partial M_{t_2}^2}{\partial \phi_d} \right)^2 + \frac{\partial \Delta V}{\partial M_{t_2}^2} \frac{\partial^2 M_{t_2}^2}{\partial \phi_d \partial \phi_d} + \frac{\partial^2 \Delta V}{\partial C_{2\theta_t}^2 \partial C_{2\theta_t}^2} \left( \frac{\partial C_{2\theta_t}^2}{\partial \phi_d} \right)^2 \\
&+ \frac{\partial \Delta V}{\partial C_{2\theta_t}^2} \frac{\partial^2 C_{2\theta_t}^2}{\partial \phi_d \partial \phi_d} + 2 \frac{\partial^2 \Delta V}{\partial M_{t_1}^2 \partial C_{2\theta_t}^2} \frac{\partial M_{t_1}^2}{\partial \phi_d} \frac{\partial C_{2\theta_t}^2}{\partial \phi_d} + 2 \frac{\partial^2 \Delta V}{\partial C_{2\theta_t}^2 \partial M_{t_2}^2} \frac{\partial C_{2\theta_t}^2}{\partial \phi_d} \frac{\partial M_{t_2}^2}{\partial \phi_d}, \tag{A1}
\end{aligned}$$

$$\begin{aligned}
\left[ -\frac{1}{\phi_u} \frac{\partial \Delta V}{\partial \phi_u} + \frac{\partial^2 \Delta V}{\partial \phi_u \partial \phi_u} \right] \Big|_{VEV} &= -\frac{1}{v_u} \left[ \frac{\partial \Delta V}{\partial m_t^2} \frac{\partial m_t^2}{\partial \phi_u} + \frac{\partial \Delta V}{\partial M_{t_1}^2} \frac{\partial M_{t_1}^2}{\partial \phi_u} + \frac{\partial \Delta V}{\partial M_{t_2}^2} \frac{\partial M_{t_2}^2}{\partial \phi_u} \right. \\
&+ \left. \frac{\partial \Delta V}{\partial C_{2\theta_t}^2} \frac{\partial C_{2\theta_t}^2}{\partial \phi_u} \right] + \frac{\partial^2 \Delta V}{\partial m_t^2 \partial m_t^2} \left( \frac{\partial m_t^2}{\partial \phi_u} \right)^2 + \frac{\partial \Delta V}{\partial m_t^2} \frac{\partial^2 m_t^2}{\partial \phi_u \partial \phi_u} + \frac{\partial^2 \Delta V}{\partial M_{t_1}^2 \partial M_{t_1}^2} \left( \frac{\partial M_{t_1}^2}{\partial \phi_u} \right)^2 \\
&+ \frac{\partial \Delta V}{\partial M_{t_1}^2} \frac{\partial^2 M_{t_1}^2}{\partial \phi_u \partial \phi_u} + 2 \frac{\partial^2 \Delta V}{\partial M_{t_1}^2 \partial M_{t_2}^2} \frac{\partial M_{t_1}^2}{\partial \phi_u} \frac{\partial M_{t_2}^2}{\partial \phi_u} + \frac{\partial^2 \Delta V}{\partial M_{t_2}^2 \partial M_{t_2}^2} \left( \frac{\partial M_{t_2}^2}{\partial \phi_u} \right)^2 \\
&+ \frac{\partial \Delta V}{\partial M_{t_2}^2} \frac{\partial^2 M_{t_2}^2}{\partial \phi_u \partial \phi_u} + 2 \frac{\partial^2 \Delta V}{\partial m_t^2 \partial M_{t_1}^2} \frac{\partial m_t^2}{\partial \phi_u} \frac{\partial M_{t_1}^2}{\partial \phi_u} + 2 \frac{\partial^2 \Delta V}{\partial m_t^2 \partial M_{t_2}^2} \frac{\partial m_t^2}{\partial \phi_u} \frac{\partial M_{t_2}^2}{\partial \phi_u} \\
&+ \frac{\partial^2 \Delta V}{\partial C_{2\theta_t}^2 \partial C_{2\theta_t}^2} \left( \frac{\partial C_{2\theta_t}^2}{\partial \phi_u} \right)^2 + \frac{\partial \Delta V}{\partial C_{2\theta_t}^2} \frac{\partial^2 C_{2\theta_t}^2}{\partial \phi_u \partial \phi_u} + 2 \frac{\partial^2 \Delta V}{\partial m_t^2 \partial C_{2\theta_t}^2} \frac{\partial m_t^2}{\partial \phi_u} \frac{\partial C_{2\theta_t}^2}{\partial \phi_u} \\
&+ 2 \frac{\partial^2 \Delta V}{\partial M_{t_1}^2 \partial C_{2\theta_t}^2} \frac{\partial M_{t_1}^2}{\partial \phi_u} \frac{\partial C_{2\theta_t}^2}{\partial \phi_u} + 2 \frac{\partial^2 \Delta V}{\partial M_{t_2}^2 \partial C_{2\theta_t}^2} \frac{\partial M_{t_2}^2}{\partial \phi_u} \frac{\partial C_{2\theta_t}^2}{\partial \phi_u}, \tag{A2}
\end{aligned}$$

$$\begin{aligned}
\left[ -\frac{1}{\phi_\eta} \frac{\partial \Delta V}{\partial \phi_\eta} + \frac{\partial^2 \Delta V}{\partial \phi_\eta \partial \phi_\eta} \right] \Big|_{VEV} &= -\frac{1}{v_\eta} \left[ \frac{\partial \Delta V}{\partial M_{t_1}^2} \frac{\partial M_{t_1}^2}{\partial \phi_\eta} + \frac{\partial \Delta V}{\partial M_{t_2}^2} \frac{\partial M_{t_2}^2}{\partial \phi_\eta} + \frac{\partial \Delta V}{\partial C_{2\theta_t}^2} \frac{\partial C_{2\theta_t}^2}{\partial \phi_\eta} \right] \\
&+ \frac{\partial^2 \Delta V}{\partial M_{t_1}^2 \partial M_{t_1}^2} \left( \frac{\partial M_{t_1}^2}{\partial \phi_\eta} \right)^2 + \frac{\partial \Delta V}{\partial M_{t_1}^2} \frac{\partial^2 M_{t_1}^2}{\partial \phi_\eta \partial \phi_\eta} + 2 \frac{\partial^2 \Delta V}{\partial M_{t_1}^2 \partial M_{t_2}^2} \frac{\partial M_{t_1}^2}{\partial \phi_\eta} \frac{\partial M_{t_2}^2}{\partial \phi_\eta}
\end{aligned}$$





where

$$C_{2\theta_t}^2 = 1 - \frac{2|m_{\tilde{t}_{12}}^2|^2}{(M_{\tilde{t}_1}^2 - M_{\tilde{t}_2}^2)^2}. \quad (\text{A11})$$

From the concrete expression of  $\Delta V$  defined in Eqs. (12, 13), we can obtain

$$\frac{\partial V^{(1)}}{\partial m_t^2} = -\frac{3m_t^2}{8\pi^2}(\log \frac{m_t^2}{Q^2} - 1), \quad \frac{\partial^2 V^{(1)}}{\partial m_t^2 \partial m_t^2} = -\frac{3}{8\pi^2} \log \frac{m_t^2}{Q^2}, \quad (\text{A12})$$

$$\frac{\partial V^{(1)}}{\partial M_{\tilde{t}_1}^2} = \frac{3M_{\tilde{t}_1}^2}{16\pi^2}(\log \frac{M_{\tilde{t}_1}^2}{Q^2} - 1), \quad \frac{\partial^2 V^{(1)}}{\partial M_{\tilde{t}_1}^2 \partial M_{\tilde{t}_1}^2} = \frac{3}{16\pi^2} \log \frac{M_{\tilde{t}_1}^2}{Q^2}, \quad (\text{A13})$$

$$\frac{\partial V^{(1)}}{\partial M_{\tilde{t}_2}^2} = \frac{3M_{\tilde{t}_2}^2}{16\pi^2}(\log \frac{M_{\tilde{t}_2}^2}{Q^2} - 1), \quad \frac{\partial^2 V^{(1)}}{\partial M_{\tilde{t}_2}^2 \partial M_{\tilde{t}_2}^2} = \frac{3}{16\pi^2} \log \frac{M_{\tilde{t}_2}^2}{Q^2}, \quad (\text{A14})$$

and the results of  $\partial V^{(2)}/\partial M^2$ ,  $\partial^2 V^{(2)}/(\partial M^2 \partial M^2)$  with  $M = m_t, M_{\tilde{t}_1}, M_{\tilde{t}_2}$  can be found in the appendix of Ref. [58]. The derivatives of  $m_t^2, M_{\tilde{t}_1}^2, M_{\tilde{t}_2}^2, C_{2\theta_t}^2$  over  $\phi_i$ , ( $i = d, u, \eta, \bar{\eta}$ ) can be written as

$$\frac{\partial m_t^2}{\partial \phi_u} = Y_t^2 v_u, \quad \frac{\partial^2 m_t^2}{\partial \phi_u \partial \phi_u} = Y_t^2, \quad (\text{A15})$$

$$\frac{\partial m_{\tilde{t}_{1,2}}^2}{\partial \phi_d} = \frac{1}{8} G^2 \phi_d \pm \frac{\frac{1}{24} G_1^2 \phi_d M_{\tilde{t}_{LR}}^2 + Y_t \mu m_{\tilde{t}_{12}}^2}{\{M_{\tilde{t}_{LR}}^4 + 2m_{\tilde{t}_{12}}^4\}^{1/2}},$$

$$\frac{\partial^2 m_{\tilde{t}_{1,2}}^2}{\partial \phi_d \partial \phi_d} = \frac{1}{8} G^2 \mp \frac{2\left\{-\frac{1}{24} G_1^2 v_d M_{\tilde{t}_{LR}}^2 + Y_t \mu m_{\tilde{t}_{12}}^2\right\}^2}{\{M_{\tilde{t}_{LR}}^4 + 2m_{\tilde{t}_{12}}^4\}^{3/2}} \mp \frac{\frac{1}{24} G_1^2 M_{\tilde{t}_{LR}}^2 - \frac{2}{24^2} G_1^4 v_d^2 - (\mu Y_t)^2}{\{M_{\tilde{t}_{LR}}^4 + 2m_{\tilde{t}_{12}}^4\}^{1/2}}, \quad (\text{A16})$$

$$\frac{\partial m_{\tilde{t}_{1,2}}^2}{\partial \phi_u} = (Y_t^2 - \frac{1}{8} G^2) v_u \pm \frac{\frac{1}{24} G_1^2 v_u M_{\tilde{t}_{LR}}^2 - Y_t A_t m_{\tilde{t}_{12}}^2}{\{M_{\tilde{t}_{LR}}^4 + 2m_{\tilde{t}_{12}}^4\}^{1/2}},$$

$$\frac{\partial^2 m_{\tilde{t}_{1,2}}^2}{\partial \phi_u \partial \phi_u} = Y_t^2 - \frac{1}{8} G^2 \mp \frac{2\left\{\frac{1}{24} G_1^2 v_u M_{\tilde{t}_{LR}}^2 - Y_t A_t m_{\tilde{t}_{12}}^2\right\}^2}{\{M_{\tilde{t}_{LR}}^4 + 2m_{\tilde{t}_{12}}^4\}^{3/2}} \pm \frac{\frac{1}{24} G_1^2 M_{\tilde{t}_{LR}}^2 + \frac{2}{24^2} G_1^4 v_u^2 + (A_t Y_t)^2}{\{M_{\tilde{t}_{LR}}^4 + 2m_{\tilde{t}_{12}}^4\}^{1/2}}, \quad (\text{A17})$$

$$\frac{\partial m_{\tilde{t}_{1,2}}^2}{\partial \phi_\eta} = \frac{1}{4} g_B g_{YB} v_\eta \mp \frac{\frac{1}{24} G_2^2 v_\eta M_{\tilde{t}_{LR}}^2}{\{M_{\tilde{t}_{LR}}^4 + 2m_{\tilde{t}_{12}}^4\}^{1/2}},$$

$$\frac{\partial^2 m_{\tilde{t}_{1,2}}^2}{\partial \phi_\eta \partial \phi_\eta} = \frac{1}{4} g_B g_{YB} \pm \frac{(\frac{1}{12} G_2^2 m_{\tilde{t}_{12}}^2 v_\eta)^2}{\{M_{\tilde{t}_{LR}}^4 + 2m_{\tilde{t}_{12}}^4\}^{3/2}} \mp \frac{\frac{1}{24} G_2^2 M_{\tilde{t}_{LR}}^2}{\{M_{\tilde{t}_{LR}}^4 + 2m_{\tilde{t}_{12}}^4\}^{1/2}}, \quad (\text{A18})$$

$$\frac{\partial m_{\tilde{t}_{1,2}}^2}{\partial \phi_{\bar{\eta}}} = -\frac{1}{4} g_B g_{YB} v_{\bar{\eta}} \pm \frac{\frac{1}{24} G_2^2 v_{\bar{\eta}} M_{\tilde{t}_{LR}}^2}{\{M_{\tilde{t}_{LR}}^4 + 2m_{\tilde{t}_{12}}^4\}^{1/2}},$$



$$\frac{\partial^2 m_{\bar{t}1,2}^2}{\partial \phi_{\bar{\eta}} \partial \phi_{\bar{\eta}}} = -\frac{1}{4} g_B g_{YB} \pm \frac{(\frac{1}{12} G_2^2 m_{\bar{t}12}^2 v_{\bar{\eta}})^2}{\{M_{\bar{t}LR}^4 + 2m_{\bar{t}12}^4\}^{3/2}} \pm \frac{\frac{1}{24} G_2^2 M_{\bar{t}LR}^2}{\{M_{\bar{t}LR}^4 + 2m_{\bar{t}12}^4\}^{1/2}}, \quad (\text{A19})$$

$$\frac{\partial^2 m_{\bar{t}1,2}^2}{\partial \phi_d \partial \phi_u} = \mp (Y_t A_t M_{\bar{t}LR}^2 + \frac{1}{12} G_1^2 v_u m_{\bar{t}12}^2) (Y_t \mu M_{\bar{t}LR}^2 + \frac{1}{12} G_1^2 v_d m_{\bar{t}12}^2) / (M_{\bar{t}LR}^4 + 2m_{\bar{t}12}^4)^{3/2}, \quad (\text{A20})$$

$$\frac{\partial^2 m_{\bar{t}1,2}^2}{\partial \phi_d \partial \phi_{\eta}} = \pm \frac{1}{12} G_2^2 v_{\eta} m_{\bar{t}12}^2 \{Y_t \mu M_{\bar{t}LR}^2 + \frac{1}{12} G_1^2 v_d m_{\bar{t}12}^2\} / \{M_{\bar{t}LR}^4 + 2m_{\bar{t}12}^4\}^{3/2}, \quad (\text{A21})$$

$$\frac{\partial^2 m_{\bar{t}1,2}^2}{\partial \phi_d \partial \phi_{\bar{\eta}}} = \mp \frac{1}{12} G_2^2 v_{\bar{\eta}} m_{\bar{t}12}^2 \{Y_t \mu M_{\bar{t}LR}^2 + \frac{1}{12} G_1^2 v_d m_{\bar{t}12}^2\} / \{M_{\bar{t}LR}^4 + 2m_{\bar{t}12}^4\}^{3/2}, \quad (\text{A22})$$

$$\frac{\partial^2 m_{\bar{t}1,2}^2}{\partial \phi_u \partial \phi_{\eta}} = \mp \frac{1}{12} G_2^2 v_{\eta} m_{\bar{t}12}^2 \{Y_t A_t M_{\bar{t}LR}^2 + \frac{1}{12} G_1^2 v_u m_{\bar{t}12}^2\} / \{M_{\bar{t}LR}^4 + 2m_{\bar{t}12}^4\}^{3/2}, \quad (\text{A23})$$

$$\frac{\partial^2 m_{\bar{t}1,2}^2}{\partial \phi_u \partial \phi_{\bar{\eta}}} = \pm \frac{1}{12} G_2^2 v_{\bar{\eta}} m_{\bar{t}12}^2 \{Y_t A_t M_{\bar{t}LR}^2 + \frac{1}{12} G_1^2 v_u m_{\bar{t}12}^2\} / \{M_{\bar{t}LR}^4 + 2m_{\bar{t}12}^4\}^{3/2}, \quad (\text{A24})$$

$$\frac{\partial^2 m_{\bar{t}1,2}^2}{\partial \phi_{\eta} \partial \phi_{\bar{\eta}}} = \mp \frac{(\frac{1}{12} G_2^2 m_{\bar{t}12}^2)^2 v_{\eta} v_{\bar{\eta}}}{\{M_{\bar{t}LR}^4 + 2m_{\bar{t}12}^4\}^{3/2}}, \quad (\text{A25})$$

$$\begin{aligned} \frac{\partial C_{2\bar{\theta}t}^2}{\partial \phi_d} &= \frac{4m_{\bar{t}12}^2}{(M_{\bar{t}1}^2 - M_{\bar{t}2}^2)^3} \left[ m_{\bar{t}12}^2 \left( \frac{\partial M_{\bar{t}1}^2}{\partial \phi_d} - \frac{\partial M_{\bar{t}2}^2}{\partial \phi_d} \right) - (M_{\bar{t}1}^2 - M_{\bar{t}2}^2) \frac{\partial m_{\bar{t}12}^2}{\partial \phi_d} \right], \\ \frac{\partial^2 C_{2\bar{\theta}t}^2}{\partial \phi_d \partial \phi_d} &= \frac{4}{(M_{\bar{t}1}^2 - M_{\bar{t}2}^2)^4} \left[ (M_{\bar{t}1}^2 - M_{\bar{t}2}^2) \frac{\partial m_{\bar{t}12}^2}{\partial \phi_d} - 3m_{\bar{t}12}^2 \left( \frac{\partial M_{\bar{t}1}^2}{\partial \phi_d} - \frac{\partial M_{\bar{t}2}^2}{\partial \phi_d} \right) \right] \left[ m_{\bar{t}12}^2 \left( \frac{\partial M_{\bar{t}1}^2}{\partial \phi_d} \right. \right. \\ &\quad \left. \left. - \frac{\partial M_{\bar{t}2}^2}{\partial \phi_d} \right) - (M_{\bar{t}1}^2 - M_{\bar{t}2}^2) \frac{\partial m_{\bar{t}12}^2}{\partial \phi_d} \right] + \frac{4m_{\bar{t}12}^2}{(M_{\bar{t}1}^2 - M_{\bar{t}2}^2)^3} \left[ m_{\bar{t}12}^2 \left( \frac{\partial^2 M_{\bar{t}1}^2}{\partial \phi_d \partial \phi_d} - \frac{\partial^2 M_{\bar{t}2}^2}{\partial \phi_d \partial \phi_d} \right) \right], \quad (\text{A26}) \end{aligned}$$

$$\begin{aligned} \frac{\partial C_{2\bar{\theta}t}^2}{\partial \phi_u} &= \frac{4m_{\bar{t}12}^2}{(M_{\bar{t}1}^2 - M_{\bar{t}2}^2)^3} \left[ m_{\bar{t}12}^2 \left( \frac{\partial M_{\bar{t}1}^2}{\partial \phi_u} - \frac{\partial M_{\bar{t}2}^2}{\partial \phi_u} \right) - (M_{\bar{t}1}^2 - M_{\bar{t}2}^2) \frac{\partial m_{\bar{t}12}^2}{\partial \phi_u} \right], \\ \frac{\partial^2 C_{2\bar{\theta}t}^2}{\partial \phi_u \partial \phi_u} &= \frac{4}{(M_{\bar{t}1}^2 - M_{\bar{t}2}^2)^4} \left[ (M_{\bar{t}1}^2 - M_{\bar{t}2}^2) \frac{\partial m_{\bar{t}12}^2}{\partial \phi_u} - 3m_{\bar{t}12}^2 \left( \frac{\partial M_{\bar{t}1}^2}{\partial \phi_u} - \frac{\partial M_{\bar{t}2}^2}{\partial \phi_u} \right) \right] \left[ m_{\bar{t}12}^2 \left( \frac{\partial M_{\bar{t}1}^2}{\partial \phi_u} \right. \right. \\ &\quad \left. \left. - \frac{\partial M_{\bar{t}2}^2}{\partial \phi_u} \right) - (M_{\bar{t}1}^2 - M_{\bar{t}2}^2) \frac{\partial m_{\bar{t}12}^2}{\partial \phi_u} \right] + \frac{4m_{\bar{t}12}^2}{(M_{\bar{t}1}^2 - M_{\bar{t}2}^2)^3} \left[ m_{\bar{t}12}^2 \left( \frac{\partial^2 M_{\bar{t}1}^2}{\partial \phi_u \partial \phi_u} - \frac{\partial^2 M_{\bar{t}2}^2}{\partial \phi_u \partial \phi_u} \right) \right], \quad (\text{A27}) \end{aligned}$$

$$\begin{aligned} \frac{\partial C_{2\bar{\theta}t}^2}{\partial \phi_{\eta}} &= \frac{4m_{\bar{t}12}^2}{(M_{\bar{t}1}^2 - M_{\bar{t}2}^2)^3} \left[ m_{\bar{t}12}^2 \left( \frac{\partial M_{\bar{t}1}^2}{\partial \phi_{\eta}} - \frac{\partial M_{\bar{t}2}^2}{\partial \phi_{\eta}} \right) \right], \\ \frac{\partial^2 C_{2\bar{\theta}t}^2}{\partial \phi_{\eta} \partial \phi_{\eta}} &= \frac{4}{(M_{\bar{t}1}^2 - M_{\bar{t}2}^2)^4} \left[ -3m_{\bar{t}12}^2 \left( \frac{\partial M_{\bar{t}1}^2}{\partial \phi_{\eta}} - \frac{\partial M_{\bar{t}2}^2}{\partial \phi_{\eta}} \right) \right] \left[ m_{\bar{t}12}^2 \left( \frac{\partial M_{\bar{t}1}^2}{\partial \phi_{\eta}} - \frac{\partial M_{\bar{t}2}^2}{\partial \phi_{\eta}} \right) \right] \\ &\quad + \frac{4m_{\bar{t}12}^2}{(M_{\bar{t}1}^2 - M_{\bar{t}2}^2)^3} \left[ m_{\bar{t}12}^2 \left( \frac{\partial^2 M_{\bar{t}1}^2}{\partial \phi_{\eta} \partial \phi_{\eta}} - \frac{\partial^2 M_{\bar{t}2}^2}{\partial \phi_{\eta} \partial \phi_{\eta}} \right) \right], \quad (\text{A28}) \end{aligned}$$



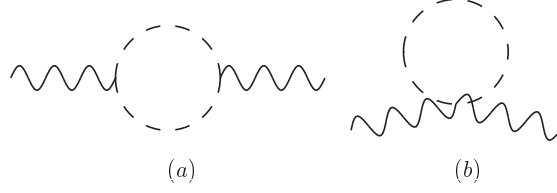


FIG. 5: The Feynman diagrams contributing to the  $\gamma$ ,  $W$ ,  $Z$  self-energy and  $\gamma - Z$  mixing, where the loop particles are squarks.

$$-\frac{\partial m_{\tilde{t}_{12}}^2}{\partial \phi_u} \left( \frac{\partial M_{\tilde{t}_1}^2}{\partial \phi_{\bar{\eta}}} - \frac{\partial M_{\tilde{t}_2}^2}{\partial \phi_{\bar{\eta}}} \right), \quad (\text{A34})$$

$$\begin{aligned} \frac{\partial^2 C_{2\bar{\theta}_i}^2}{\partial \phi_\eta \partial \phi_{\bar{\eta}}} &= \frac{4}{(M_{\tilde{t}_1}^2 - M_{\tilde{t}_2}^2)^4} \left[ -3m_{\tilde{t}_{12}}^2 \left( \frac{\partial M_{\tilde{t}_1}^2}{\partial \phi_{\bar{\eta}}} - \frac{\partial M_{\tilde{t}_2}^2}{\partial \phi_{\bar{\eta}}} \right) \right] \left[ m_{\tilde{t}_{12}}^2 \left( \frac{\partial M_{\tilde{t}_1}^2}{\partial \phi_\eta} - \frac{\partial M_{\tilde{t}_2}^2}{\partial \phi_\eta} \right) \right] \\ &+ \frac{4m_{\tilde{t}_{12}}^2}{(M_{\tilde{t}_1}^2 - M_{\tilde{t}_2}^2)^3} \left[ m_{\tilde{t}_{12}}^2 \left( \frac{\partial^2 M_{\tilde{t}_1}^2}{\partial \phi_\eta \partial \phi_{\bar{\eta}}} - \frac{\partial^2 M_{\tilde{t}_2}^2}{\partial \phi_\eta \partial \phi_{\bar{\eta}}} \right) \right], \end{aligned} \quad (\text{A35})$$

where

$$\begin{aligned} G^2 &= g_1^2 + g_2^2 + g_{YB}^2, \quad G_1^2 = 5g_1^2 - 3g_2^2 + 5g_{YB}^2 + 2g_B g_{YB}, \quad G_2^2 = 4g_B^2 + 10g_B g_{YB}, \\ m_{\tilde{t}_{12}}^2 &= Y_t(\mu v_d - A_t v_u), \\ M_{\tilde{t}_{LR}}^2 &= \frac{1}{24} [24(M_Q^2 - M_U^2) + G_1^2(v_u^2 - v_d^2) + G_2^2(v_\eta^2 - v_{\bar{\eta}}^2)]. \end{aligned} \quad (\text{A36})$$

## Appendix B: The contributions from squarks to $S$ , $T$ , $U$ parameters in the B-LSSM.

The one-loop diagrams contributing to the  $\gamma$ ,  $W$ ,  $Z$  self-energy and  $\gamma - Z$  mixing are plotted in Fig. 5, where the loop particles are squarks. Since the  $Z - Z'$  mixing is limited to be very small ( $\lesssim 10^{-4}$ ) experimentally, we can neglect the  $Z - Z'$  mixing contributions safely in the calculation. Then the results can be written as

$$\begin{aligned} \Pi_{ZZ} &= \frac{1}{16\pi^2} (C_{Z\bar{Q}_i\bar{Q}_j})^2 \left[ I_1(M_{\bar{Q}_i}^2, M_{\bar{Q}_j}^2) + I_2(M_{\bar{Q}_i}^2, M_{\bar{Q}_j}^2) q^2 \right] - \\ &\frac{1}{16\pi^2} (C_{ZZ\bar{Q}_i\bar{Q}_i}) I_3(M_{\bar{Q}_i}^2), \end{aligned} \quad (\text{B1})$$

$$\begin{aligned} \Pi_{WW} &= \frac{1}{16\pi^2} (C_{W\bar{U}_i\bar{D}_j})^2 \left[ I_1(M_{\bar{U}_i}^2, M_{\bar{D}_j}^2) + I_2(M_{\bar{U}_i}^2, M_{\bar{D}_j}^2) q^2 \right] - \\ &\frac{1}{16\pi^2} (C_{WW\bar{Q}_i\bar{Q}_i}) I_3(M_{\bar{Q}_i}^2), \end{aligned} \quad (\text{B2})$$

$$\Pi_{\gamma\gamma} = \frac{1}{16\pi^2} (C_{\gamma\tilde{Q}_i\tilde{Q}_j})^2 I_2(M_{\tilde{Q}_i}^2, M_{\tilde{Q}_j}^2) q^2, \quad (\text{B3})$$

$$\Pi_{\gamma Z} = \frac{1}{16\pi^2} (C_{\gamma\tilde{Q}_i\tilde{Q}_j} C_{Z\tilde{Q}_i\tilde{Q}_j}) I_2(M_{\tilde{Q}_i}^2, M_{\tilde{Q}_j}^2) q^2, \quad (\text{B4})$$

where  $C_{abc}$  and  $C_{abcd}$  denote the coupling constants of fields  $abc$ ,  $abcd$  respectively,  $M_{\tilde{Q}_i}$  denotes the squark mass,  $M_{\tilde{U}_i}$  denotes the up-squark mass,  $M_{\tilde{D}_i}$  denotes the down-squark mass, and

$$I_1(x, y) = x(\text{div} - \ln x) + y(\text{div} - \ln y) + f(x, y), \quad (\text{B5})$$

$$I_2(x, y) = \frac{1}{18(x-y)^2} \left[ (x+y)^2 + 8xy + 6x^2 \ln x + 6y^2 \ln y - \frac{12xy}{x-y} (x \ln x - y \ln y) \right], \quad (\text{B6})$$

$$I_3(x) = x(\text{div} - \ln x), \quad (\text{B7})$$

where

$$\text{div} \equiv \frac{2}{4-d} - \gamma + 1 + \ln(4\pi). \quad (\text{B8})$$

Then the  $S$ ,  $T$ ,  $U$  parameters [72, 73] at one-loop level in the B-LSSM can be written as

$$\begin{aligned} \hat{S} &= -\frac{c_W}{s_W} (c_W^2 \Pi'_{\gamma Z} - s_W^2 \Pi'_{\gamma Z} + c_W s_W \Pi'_{\gamma\gamma} - c_W s_W \Pi'_{ZZ}), \\ \hat{T} &= \frac{\Pi_{33} - \Pi_{WW}}{M_W^2} = -\frac{1}{M_W^2} (c_W^2 \Pi_{ZZ} + s_W^2 \Pi_{\gamma\gamma} + 2s_W c_W \Pi_{\gamma Z} - \Pi_{WW}), \\ \hat{U} &= c_W^2 \Pi'_{ZZ} + s_W^2 \Pi'_{\gamma\gamma} + 2s_W c_W \Pi'_{\gamma Z} - \Pi'_{WW}, \end{aligned} \quad (\text{B9})$$

where  $\Pi'_{V_1 V_2}$  denotes  $\partial \Pi_{V_1 V_2} / \partial q^2$  with  $V_1 V_2$  denoting  $\gamma\gamma$ ,  $ZZ$ ,  $WW$ ,  $\gamma Z$ .

## Acknowledgments

The work has been supported by the National Natural Science Foundation of China (NNSFC) with Grants No. 12075074, No. 12235008, Hebei Natural Science Foundation for Distinguished Young Scholars with Grant No. A2022201017, No. A2023201041, Natural Science Foundation of Guangxi Autonomous Region with Grant No. 2022GXNSFDA035068,

and the youth top-notch talent support program of the Hebei Province.

---

- [1] S. Chatrchyan *et al.* [CMS], Phys. Lett. B **716**, 30-61 (2012).
- [2] G. Aad *et al.* [ATLAS], Phys. Lett. B **716**, 1-29 (2012).
- [3] A. Tumasyan *et al.* [CMS], Nature **607**, no.7917, 60-68 (2022).
- [4] [ATLAS], Nature **607**, no.7917, 52-59 (2022) [erratum: Nature **612**, no.7941, E24 (2022)].
- [5] [CMS], CMS-PAS-HIG-14-037.
- [6] A. M. Sirunyan *et al.* [CMS], Phys. Lett. B **793**, 320-347 (2019).
- [7] C. Arcangeletti. on behalf of ATLAS collaboration, LHC Seminar, 7th of June, 2023.
- [8] [ATLAS], ATLAS-CONF-2018-025.
- [9] A. Tumasyan *et al.* [CMS], JHEP **07**, 073 (2023).
- [10] [CMS], CMS-PAS-HIG-20-002.
- [11] R. Barate *et al.* [LEP Working Group for Higgs boson searches, ALEPH, DELPHI, L3 and OPAL], Phys. Lett. B **565**, 61-75 (2003).
- [12] S. Moretti and S. Munir, Eur. Phys. J. C **47**, 791-803 (2006).
- [13] U. Ellwanger, Phys. Lett. B **698**, 293-296 (2011).
- [14] J. Cao, Z. Heng, T. Liu and J. M. Yang, Phys. Lett. B **703**, 462-468 (2011).
- [15] D. Albornoz Vasquez, G. Belanger, C. Boehm, J. Da Silva, P. Richardson and C. Wymant, Phys. Rev. D **86**, 035023 (2012).
- [16] U. Ellwanger and C. Hugonie, Adv. High Energy Phys. **2012**, 625389 (2012).
- [17] F. Boudjema and G. D. La Rochelle, Phys. Rev. D **86**, 115007 (2012).
- [18] K. Schmidt-Hoberg and F. Staub, JHEP **10**, 195 (2012).
- [19] M. Badziak, M. Olechowski and S. Pokorski, JHEP **06**, 043 (2013).
- [20] M. Badziak, M. Olechowski and S. Pokorski, PoS **EPS-HEP2013**, 257 (2013).
- [21] R. Barbieri, D. Buttazzo, K. Kannike, F. Sala and A. Tesi, Phys. Rev. D **88**, 055011 (2013).
- [22] J. W. Fan, J. Q. Tao, Y. Q. Shen, G. M. Chen, H. S. Chen, S. Gascon-Shotkin, M. Lethuillier, L. Sgandurra and P. Soulet, Chin. Phys. C **38**, 073101 (2014).
- [23] C. T. Potter, Eur. Phys. J. C **76**, no.1, 44 (2016).

- [24] U. Ellwanger and M. Rodriguez-Vazquez, *JHEP* **02**, 096 (2016).
- [25] J. Cao, X. Guo, Y. He, P. Wu and Y. Zhang, *Phys. Rev. D* **95**, no.11, 116001 (2017).
- [26] J. Cao, X. Jia, Y. Yue, H. Zhou and P. Zhu, *Phys. Rev. D* **101**, no.5, 055008 (2020).
- [27] J. Cao, X. Jia, J. Lian and L. Meng, [arXiv:2310.08436 [hep-ph]].
- [28] J. Cao, X. Jia and J. Lian, [arXiv:2402.15847 [hep-ph]].
- [29] T. Biekötter, M. Chakraborti and S. Heinemeyer, *Eur. Phys. J. C* **80**, no.1, 2 (2020).
- [30] T. Biekötter and M. O. Olea-Romacho, *JHEP* **10**, 215 (2021).
- [31] T. Biekötter, A. Grohsjean, S. Heinemeyer, C. Schwanenberger and G. Weiglein, *Eur. Phys. J. C* **82**, no.2, 178 (2022).
- [32] S. Heinemeyer, C. Li, F. Lika, G. Moortgat-Pick and S. Paasch, *Phys. Rev. D* **106**, no.7, 075003 (2022).
- [33] T. Biekötter, S. Heinemeyer and G. Weiglein, *JHEP* **08**, 201 (2022).
- [34] T. Biekötter, S. Heinemeyer and G. Weiglein, *Eur. Phys. J. C* **83**, no.5, 450 (2023).
- [35] T. Biekötter, S. Heinemeyer and G. Weiglein, [arXiv:2303.12018 [hep-ph]].
- [36] D. Azevedo, T. Biekötter and P. M. Ferreira, [arXiv:2305.19716 [hep-ph]].
- [37] J. A. Aguilar-Saavedra, H. B. Câmara, F. R. Joaquim and J. F. Seabra, [arXiv:2307.03768 [hep-ph]].
- [38] D. Sachdeva and S. Sadhukhan, *Phys. Rev. D* **101**, no.5, 055045 (2020).
- [39] T. Biekötter, S. Heinemeyer and C. Muñoz, *Eur. Phys. J. C* **78**, no.6, 504 (2018).
- [40] T. Biekötter, S. Heinemeyer and C. Muñoz, *Eur. Phys. J. C* **79**, no.8, 667 (2019).
- [41] S. Ashanujjaman, S. Banik, G. Coloretti, A. Crivellin, B. Mellado and A. T. Mulaudzi, [arXiv:2306.15722 [hep-ph]].
- [42] A. Azatov, R. Contino and J. Galloway, *JHEP* **04**, 127 (2012).
- [43] S. Heinemeyer and T. Stefaniak, *PoS CHARGED2018*, 016 (2019).
- [44] S. Khalil and H. Okada, *Phys. Rev. D* **79**, 083510 (2009).
- [45] A. Elsayed, S. Khalil and S. Moretti, *Phys. Lett. B* **715**, 208-213 (2012).
- [46] A. Elsayed, S. Khalil, S. Moretti and A. Moursy, *Phys. Rev. D* **87**, no.5, 053010 (2013).
- [47] W. Abdallah, A. Hammad, S. Khalil and S. Moretti, *Phys. Rev. D* **95**, no.5, 055019 (2017).
- [48] S. Khalil and S. Moretti, *Rept. Prog. Phys.* **80**, no.3, 036201 (2017).

- [49] L. Delle Rose, S. Khalil, S. J. D. King, S. Kulkarni, C. Marzo, S. Moretti and C. S. Un, JHEP **07**, 100 (2018).
- [50] J. L. Yang, T. F. Feng and H. B. Zhang, J. Phys. G **47**, no.5, 055004 (2020).
- [51] J. L. Yang, H. B. Zhang, C. X. Liu, X. X. Dong and T. F. Feng, JHEP **08**, 086 (2021).
- [52] A. A. Abdelalim, B. Das, S. Khalil and S. Moretti, Nucl. Phys. B **985**, 116013 (2022).
- [53] S. Iguro, T. Kitahara and Y. Omura, Eur. Phys. J. C **82**, no.11, 1053 (2022).
- [54] J. L. Yang, T. F. Feng, Y. L. Yan, W. Li, S. M. Zhao and H. B. Zhang, Phys. Rev. D **99**, no.1, 015002 (2019).
- [55] R. J. Zhang, Phys. Lett. B **447**, 89-97 (1999).
- [56] J. R. Espinosa and R. J. Zhang, JHEP **03**, 026 (2000).
- [57] G. Degrassi, P. Slavich and F. Zwirner, Nucl. Phys. B **611**, 403-422 (2001).
- [58] G. Degrassi and P. Slavich, Nucl. Phys. B **825**, 119-150 (2010).
- [59] R. L. Workman *et al.* [Particle Data Group], PTEP **2022**, 083C01 (2022).
- [60] P. Bechtle, H. E. Haber, S. Heinemeyer, O. Stål, T. Stefaniak, G. Weiglein and L. Zeune, Eur. Phys. J. C **77**, 67 (2017).
- [61] A. Djouadi, J. Kalinowski and M. Spira, Comput. Phys. Commun. **108**, 56-74 (1998).
- [62] ATLAS Collaboration, Report No. ATLAS-CONF-2016-045.
- [63] G. Cacciapaglia, C. Csaki, G. Marandella, and A. Strumia, Phys.Rev. D **74**, 033011 (2006) [hep-ph/0604111] .
- [64] M. Carena, A. Daleo, B. A. Dobrescu and T. M. P. Tait, Phys. Rev. D **70**, 093009 (2004) [hep-ph/0408098].
- [65] G. Cacciapaglia, C. Csaki, G. Marandella and A. Strumia, Phys. Rev. D **74**, 033011 (2006).
- [66] J. L. Yang, Z. F. Ge, X. Y. Yang, S. K. Cui and T. F. Feng, [arXiv:2308.05304 [hep-ph]].
- [67] Lorenzo Basso, Adv. High Energy Phys. **2015**, 12 (2015).
- [68] J. L. Yang, T. F. Feng, H. B. Zhang, R. F. Zhu and S. M. Zhao, Eur. Phys. J. C **78**, 714 (2018).
- [69] ATLAS Collab., Phys. Rev. D **87**, 012008 (2013).
- [70] CMS Collab., JHEP **1210**, 018 (2012).
- [71] C. S. Un and O. Ozdal, Phys. Rev. D **93**, 055024 (2016) [arXiv:1601.02494 [hep-ph]].

- [72] M. E. Peskin and T. Takeuchi, Phys. Rev. D **46**, 381-409 (1992).
- [73] J. M. Yang and Y. Zhang, Sci. Bull. **67**, 1430-1436 (2022).